UV Laser Photolysis of Disiloxanes for Chemical Vapor Deposition of Nano-Textured Silicones

Josef Pola,*,† Anna Galíková,† Aftanas Galík,† Vratislav Blechta,† Zdeněk Bastl,‡ Jan Šubrt,§ and Akihiko Ouchi||

Institute of Chemical Process Fundamentals, Academy of Sciences of the Czech Republic, 165 02 Prague, Czech Republic, J. Heyrovský Institute of Physical Chemistry, Academy of Sciences of the Czech Republic, 182 23 Prague 8, Czech Republic, Institute of Inorganic Chemistry, Academy of Sciences of the Czech Republic 250 68 Řež near Prague, Czech Republic, and National Institute of Materials and Chemical Research, AIST, MITI, Tsukuba, Ibaraki 305, Japan

Received April 12, 2001. Revised Manuscript Received August 28, 2001

Gas-phase photolysis of methyldisiloxanes $[(CH_3)_nH_{3-n}Si]_2O$ ($n = 1-3$) has been achieved for the first time through absorption of ArF laser radiation at 193 nm and has been shown to yield C_1-C_2 hydrocarbons (major volatile products), methylsilanes (minor volatile products), and solid methylsilicones with their H(Si) content and Si/O ratio reflecting those of the parent compounds. The identified volatile and solid products are compatible with a number of reactions occurring within less than 1 ms in a narrow region of the gaseous sample maintained at room temperature. These reactions are discussed. The solid deposited materials were characterized by FTIR, NMR, UV, and XP spectroscopy, electron microscopy, and thermal gravimetry. They were revealed to contain all possible $SiC_xH_yO_z$ ($x + y + z = 4$) compositions, to possess nanometer-sized texture, and to be thermally more stable than linear poly(dialkylsiloxanes).

1. Introduction

Silicon oxycarbides have recently been paid much attention because of their significance in applied materials research (e.g., refs 1−4). Various Si/C/O and Si/C/H/O phases were produced by pyrolysis of polysiloxanes (e.g., refs 5−7), polysiloxane gels (e.g., refs 8 and 9), pyrolytic laser-aerosol interaction,[10] and plasma[11,12] or laser (e.g., refs 13−15) interaction with gaseous organosilanes.

We have recently shown[16−18] that IR laser-induced thermolysis of volatile hydridodisiloxanes in the gas phase can lead to chemical vapor deposition (CVD) of solid nano-structured silicones with Si−H bonds in their backbone. These materials can[19,20] be chemically converted into macromolecules with other functional groups or act as suitable precursors for Si/C/O or Si/O phases.

Also, examination of UV laser photolysis of volatile disiloxanes is of interest because it can yield CVD of materials different from those obtained by IR laser photolysis. It is known[21,22] that the UV photolysis of Si−O bond-containing saturated organosilanes at wavelengths below 200 nm is controlled by cleavage of weak C−Si bonds. We have briefly reported on UV laser-induced photolysis of disiloxane[23] ($H_3SiOSiH_3$) and 1,3-dimethyldisiloxane[24] ($CH_3H_2SiOSiH_2CH_3$).

* To whom correspondence should be addressed. Tel: 420-2-20390308. Fax: 420-2-20920661. E-mail: pola@icpf.cas.cz.
† Institute of Chemical Process Fundamentals.
‡ J. Heyrovský Institute of Physical Chemistry.
|| Institute of Inorganic Chemistry.
§ National Institute of Materials and Chemical Research.

(1) Hurwitz, F. I.; Heimann, P.; Farmer, S. C.; Hembree, D. M. *J. Mater. Sci.* **1993**, *28*, 6622 and references therein.
(2) Breval, E.; Hammond, H.; Pantano, C. G. *J. Am. Ceram. Soc.* **1994**, *77*, 3012.
(3) Soraru, G. D.; Liu, Q.; Interrante, L. V.; Apple, T. *Chem. Mater.* **1998**, *10*, 4047.
(4) Bois, L.; Maquet, J.; Babonneau, F.; Mutin, H.; Bahloul, D. *Chem. Mater.* **1994**, *6*, 796.
(5) Wilson, A. M.; Zank, G.; Eguchi, K.; Xing, W.; Yates, B.; Dahn, J. R. *Chem. Mater.* **1997**, *9*, 1601.
(6) Mantz, R. A.; Jones, P. F.; Chaffee, K. P.; Lichtenhan, J. D.; Gilman, J. W.; Ismail, I. M. K.; Burmeister, M. J. *Chem. Mater.* **1996**, *8*, 1250.
(7) Kurjata, J.; Scibiorek, M.; Fortuniak, W.; Chojnowski, J. *Organometallics* **1999**, *18*, 1259.
(8) Babonneau, F. *Polyhedron* **1994**, *13*, 1123.
(9) Dire, S.; Campostrini, R.; Ceccato, R. *Chem. Mater.* **1998**, *10*, 268.
(10) Kortobi, Y. E.; Esoinose de la Caillerie, J.-B.; Legrand, A. P.; Armand, X.; Herlin, N.; Cauchetier, M. *Chem. Mater.* **1997**, *9*, 632.
(11) Fujii, T.; Yokoi, T.; Hiramatsu, M.; Nawata, M.; Hori, M.; Goto, T.; Hattori, S. *J. Vac. Sci. Technol., B* **1997**, *15*, 746.
(12) Bartella, J.; Herwig, U. *Fresenius Z. Anal. Chem.* **1993**, *346*, 351.
(13) Alexandrescu, R.; Morjan, J.; Grigoriu, C.; Bastl, Z.; Tláskal, J.; Mayer, R.; Pola, J. *Appl. Phys. A* **1988**, *46*, 768.
(14) Pola, J.; Čukanová, D.; Minárik, M.; Lyčka, A.; Tláskal, J. *J. Organomet. Chem.* **1992**, *23*, 426.
(15) Pola, J.; Morita, H. *Tetrahedron Lett.* **1997**, *38*, 7809.
(16) Pola, J.; Pokorná, D.; Bastl, Z.; Šubrt, J. *J. Anal. Appl. Pyrolysis* **1996**, *38*, 153.
(17) Pola, J.; Urbanová, M.; Dřínek, V.; Šubrt, J.; Beckers, H. *Appl. Organomet. Chem.* **1999**, *13*, 655.
(18) Pola, J.; Urbanová, M.; Bastl, Z.; Šubrt, J.; Papagiannakopoulos, P. *J. Mater. Chem.* **2000**, *10*, 1415.
(19) Sailor, M. J.; Lee, E. J. *Adv. Mater.* **1997**, *9*, 783.
(20) Buriak, J. M. *Adv. Mater.* **1999**, *11*, 265.
(21) Dalton, J. C. In *Organic Photochemistry*; Padwa, A., Ed.; M. Dekker: New York, 1985; Vol. 7, Chapter 3.
(22) Ouchi, A.; Koga, Y.; Bastl, Z.; Pola, J. *Appl. Organomet. Chem.* **1999**, *13*, 643.
(23) Pola, J.; Urbanová, M.; Bastl, Z.; Šubrt, J.; Beckers, H. *J. Mater. Chem.* **1999**, *9*, 2429.
(24) Pola, J.; Ouchi, A.; Šubrt, J.; Bastl, Z.; Sakuragi, M. *Chem. Vap. Depos.* **2001**, *7*, 19.

10.1021/cm011109o CCC: $22.00
Published on Web 12/04/2001

Table 1. Product Yields[a] in ArF Laser Photolysis of Methyldisiloxanes $[(CH_3)_nH_{3-n}Si]_2O$

$[(CH_3)_nH_{3-n}Si]_2O$	yield of hydrocarbons	yield of methylsilanes
$n = 1$	CH_4 (30−34), C_2H_2 (35−40), C_2H_4 (8), C_2H_6 (8−12), C_3H_8 (3), C_4H_x (2)	CH_3SiH_3 (3), $(CH_3)_2SiH_2$ (<1), $(CH_3)_3SiH$ (<1)
$n = 2$	CH_4 (50−55), C_2H_2 (10), C_2H_4 (8), C_2H_6 (16−20), C_3H_8 (3), C_4H_x (2)	CH_3SiH_3 (4), $(CH_3)_2SiH_2$ (2), $(CH_3)_3SiH$ (<1)
$n = 3$	CH_4 (42−45), C_2H_2 (5), C_2H_4 (10), C_2H_6 (30−35), C_3H_8 (4), C_4H_x (3)	CH_3SiH_3 (2), $(CH_3)_2SiH_2$ (2), $(CH_3)_3SiH$ (2)

[a] In mole percent, photolysis progress <10%.

In this paper, we present our results on ArF laser (193 nm) photolysis of a series of methyldisiloxanes $[(CH_3)_nH_{3-n}Si]_2O$ with $n = 1-3$, discuss formation of the final volatile products, and show that this photolysis can be used for chemical vapor deposition of solid nanotextured polysiloxanes which are thermally more stable than conventionally prepared linear polysiloxanes.

2. Experimental Section

Photolysis Experiments. Laser photolysis experiments were carried out with gaseous samples of disiloxanes $[(CH_3)_nH_{3-n}Si]_2O$ ($n = 1-3$) at 30 Torr by using a Lambda Physik LPX 210i (ArF) laser operating at 193 nm with a repetition rate of 3, 5, and 10 Hz and with a fluence of 100 mJ/cm^2 effective in the area of 3 cm^2. More efficient photolysis was achieved with a mildly focused laser beam. The gaseous samples were irradiated in a reactor (140 mL) furnished with 2 quartz windows, 2 KBr windows, and two ports, one fitted with a rubber septum and the other one connecting the reactor to a vacuum manifold. The progress of the photolysis was monitored by in situ infrared spectroscopical (Shimadzu FTIR 4000 spectrometer) measurement of diagnostic absorption bands of $[(CH_3)_nH_{3-n}Si]_2O$ ($n = 1-3$) at 1255 cm^{-1} ($n = 1$), 1425 cm^{-1} ($n = 2$), and 1420 cm^{-1} ($n = 3$) and also after addition of helium by gas chromatography (Gasukuro Kogyo model 370 chromatograph equipped with a packed 2-m long Unipak S SUS column, programmed temperature 30−150 °C, FID detector, helium carrier gas). The volatile photolytic products were identified by GC/MS spectrometry (Shimadzu QP 1000 spectrometer) and their amounts were determined by gas chromatography.

Model Compounds. 1,3-Dimethyldisiloxane was obtained by the cleavage of methyl(phenyl)silane (Gelest) with hydrogen bromide and subsequent hydrolysis of the produced bromo(methyl)silane, the procedure similar to that earlier reported for synthesis of 1,3-diorganylsiloxanes.[25] Gaseous hydrogen bromide (excess, 0.6 mole) was condensed into a 300-mL flask containing methyl(phenyl)silane (36 g, 0.30 mole) which was stirred by a magnetic bar and kept at −80 °C. The resultant mixture was stirred for an additional 4 h, and then the excess of hydrogen bromide was removed by slowly warming up the flask to room temperature. The resulting bromo(methyl)silane was hydrolyzed by 20 mL of water at −80 °C in the presence of potassium carbonate (21 g, 0.15 mole). 1,3-Dimethyldisiloxane (11 g, 0.10 mole, 67% yield) was distilled off the slurry kept at −60 °C. Sample purity was confirmed by gas chromatography and NMR spectroscopy.

1,1,3,3-Tetramethyldisiloxane and hexamethyldisiloxane (both Tokyo Kasei Co., Ltd.) were commercial samples which were degassed prior to use.

Properties of Deposits. The photodeposited materials were analyzed by X-ray photoelectron (XPS), FTIR and UV spectroscopy, transmission electron microscopy, and thermogravimetry.

The IR spectra (Shimadzu FTIR 4000 spectrometer) and UV spectra (Shimadzu UV 2100 spectrometer) were taken for materials deposited on KBr lumps and quartz plates which were housed in the reactor prior to irradiation.

The XPS measurements were carried out using ESCA 310 (Gammadata Scienta) spectrometer and AlKα (1487 eV) radiation. Calculation of the concentrations of elements was accomplished by correcting the photoelectron peak intensities for their cross-sections[26] and by accounting for the dependence of analyzer transmission and electron inelastic mean free paths on their kinetic energies.[27]

Solid-state MAS and CP MAS NMR experiments were conducted on a Bruker DSX200 NMR spectrometer in a 4-mm broadband probe. ^{13}C and ^{29}Si NMR spectra were externally referenced to the carbonyl line of glycine ($\delta = 176.03$) and to the M unit line of M8Q8 ($\delta = 11.5$), respectively. The samples were spun with spinning speed of 1600 Hz for ^{29}Si CP MAS experiments, 2500 Hz for ^{29}Si MAS experiments, and 4000 Hz for ^{13}C experiments. Relaxation delay of 60 s for all MAS experiments and 6 s for all CP MAS experiments were used. CP delays of 2 ms and 5 ms were used for ^{13}C and ^{29}Si CP MAS experiments, respectively. Usually about 1000 scans were accumulated for any of the experiments, the exception being 12000 scans for ^{13}C CP MAS experiments on the solid obtained from 1,1-dimethyldisiloxane.

SEM photographs were obtained using a Philips XL30 CP Scanning Electron Microscope and TEM photomicrographs were obtained using a Philips 201 transmission electron microscope.

Thermal analysis of the solid-laser-deposited materials (sample weight 2.5−4.5 mg) was carried out by heating the samples up to 850 °C at the rate of 3.5 °C per minute, using Cahn D-200 recording microbalances in a stream of argon. The composition of the outgoing gases was analyzed by an automatic sampling gas chromatograph Hewlett-Packard GC5890 equipped with FID and TCD detectors and Porapak P packed column (i.d. 2 mm, length 2 m). The quantification of the chromatographic data was made using streams of argon mixed with measured amounts of methane and ethyne as controlled by mass flow AFC 2600 controllers (Aalborg instruments, Inc.) The sample residue remaining on the balance pan was analyzed in a KBr pellet by FTIR spectroscopy, photoelectron spectroscopy, and electron microscopy.

3. Results

Laser Photolysis. Gaseous $[(CH_3)_nH_{3-n}Si]_2O$ ($n = 1-3$) disiloxanes were ArF laser-photolyzed despite that their absorptivity at 193 nm (in 10^{-3} Torr^{-1} cm^{-1})—2.0 ($n = 1$), 0.2 ($n = 2$), and 0.9 ($n = 3$)—is rather low. Each photolysis results in the formation of methane, ethane, ethene, propene, ethyne, and methylsilanes $(CH_3)_nSiH_{4-n}$ ($n = 1-3$) and of solid, initially white and at later stages grayish materials. The yields of these compounds within 10% photolytic progress are given in Table 1. The solid materials deposit throughout all the inside of the reactor and gradually build up on the entrance quartz window, where they cause a continuous decay of the laser power within the reactor because of their absorption at 193 nm. This makes the photolysis progress higher than 10% difficult to achieve even when the irradiation is

(25) Bisinger, P.; Paul, M.; Riede, J.; Schmidbaur, H. *Chem. Ber.* **1993**, *126*, 2579.

(26) Scofield, J. H. *J. Electron Spectrosc.* **1976**, *8*, 129.

(27) Seah, M. P.; Dench, W. A. *Surf. Interface Anal.* **1979**, *1*, 1.

Table 2. FTIR Spectra of $[(CH_3)_nH_{3-n}Si]_2O$ and Solid Materials Therefrom

	absorbance[a]/wavelength in cm^{-1}					
	$n = 1$		$n = 2$		$n = 3$	
vibration	solid material	disiloxane	solid material	disiloxane	solid material	disiloxane
ν(Si−C), $\rho(CH_3Si)$	0.50/800	0.37/765	0.67/803	0.23/780 0.18/835	0.63/797	0.08/756
δ(Si−H), $\rho(CH_3Si)$	0.56/870	1.64/920 0.60/965	0.21/908	1.27/886 0.68/908	0.90/842	0.53/852
ν(SiOSi)	1.0/1050	1.0/1086	0.86/1090 1.0/1040	1.0/1075	1.0/1100	1.0/1069
$\delta(CH_3Si)$	0.19/1260	0.17/1260	0.51/1264	0.41/1265	0.60/1256	0.37/1255
ν(Si−H)	0.26/2144	0.94/2140	0.14/2136	0.61/2125		
ν(C−H)	0.07/2960	0.07/2960	0.17/2964	0.21/2956	0.31/2960	0.21/2958

[a] Normalized to absorbance of ν(SiOSi) band.

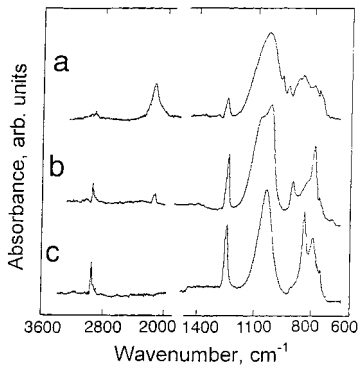

Figure 1. FTIR absorption spectra of the solid materials from $[CH_3H_2Si]_2O$ (a), $[(CH_3)_2HSi]_2O$ (b), and $[(CH_3)_3Si]_2O$ (c).

directed through both reactor windows. The irradiation periods with 3 Hz repetition frequency required for 10% photolysis of $[(CH_3)_nH_{3-n}Si]_2O$ (depletion of 2.5×10^{-5} mole) are 30 min ($n = 2$) and ca. 10−20 min ($n = 1, 3$) and reflect absorptivity of the disiloxanes as well as that of the solid-deposited materials.

Deposited Materials. The materials deposited from the individual disiloxanes have different appearances and properties. Those obtained from $[(CH_3)_nH_{3-n}Si]_2O$ ($n = 1, 2$) after one or two photolytical runs are white thin films which show very good adhesion to the glass reactor surface and which survive the tape test. The repeated photolysis yields thick coatings that can be easily removed from the surface in the form of a light grayish powder. One or two photolysis runs on $[(CH_3)_3Si]_2O$ yield white layers not adhesive to the glass surface, whereas more photolytic runs yields a slush. The slush is composed of a viscous liquid and a grayish solid. The liquid portion was revealed by mass spectroscopy to be a mixture of oligomethylsiloxanes containing 3−10 Si atoms.

All the solids are insoluble in organic solvents (diethyl ether, chloroform, and toluene), which indicates that they possess a high molecular weight or a cross-linked structure. Insight into the structure of the solid materials obtained from each disiloxane is provided by the analyses below.

Infrared Spectra. The deposited solid materials show IR absorptions (Figure 1, Table 2) typical for polymethylsiloxanes[28] which differ in the content of Si−H and CH_3−Si bonds and possess different Si/O arrangements. The ν(Si−H) band is observed only in the solids from 1,3-dimethyldisiloxane and 1,1,3,3-tetramethyldisiloxane; its normalized absorbance indicates that the content of H(Si) centers is higher in the former material. The band positions close to those of the parent disiloxanes reveal[29,30] the occurrence of H(Si)−O moieties. The normalized absorbances of the ν(C−H) and $\delta(CH_3Si)$ within each pair of the disiloxane and the solid are not significantly different and reflect similar content of the H(C) centers in the precursors and the deposits. The ratios of absorbances A[ν(C−H)]:A[ν(Si−H)] for the solids from 1,3-dimethyldisiloxane and 1,1,3,3-tetramethyldisiloxane (0.27 and 1.21, respectively) are significantly higher than the corresponding ratios for the gaseous disiloxanes (0.08 and 0.34, respectively) and imply that these deposits contain less H(Si) centers relative to H(C) centers than their precursors. These ratios allow to estimate[31] the relative concentrations of H(Si) and H(C) centers: both types of centers are almost equally present in the solid from 1,3-dimethyldisiloxane, whereas the H(C) centers are about 5 times more abundant in the solid from 1,1,3,3-tetramethyldisiloxane.

UV−Vis Spectra. UV−vis spectra of the deposits from $[(CH_3)_nH_{3-n}Si]_2O$ ($n = 1, 3$) show a similar continuous decrease of absorbance from 193 nm to higher wavelengths (Figure 2). A maximum at 220 nm and a shoulder at ∼470 nm is observed with the deposit from 1,1,3,3-tetramethyldisiloxane.

XPS Analysis. The results of the XPS analysis of the deposits reveal that the binding energies of Si (2p) electrons (Figure 3) in all samples is equal to 102.3 ± 0.1 eV, which is characteristic of dimethylsilicone polymers.[32] The surface stoichiometry of the deposits calculated from intensities of photoemission lines together with the bulk stoichiometry calculated from the EDX−SEM analysis are given in Table 3. The XPS analysis shows an equal amount of Si and O and a higher amount of C in superficial (ca. 5 nm) layers, whereas the EDX−SEM analysis reveals the Si/O and C/Si ratio is greater than 1 in the bulk material. The increased oxygen content in the topmost layers indicates that materials are oxidized at their surface. Oxidation

(28) *Infrared Structural Correlation Tables and Data Cards*; Miller, R. G. J. and Willis, H. A., Eds.; Heyden: London, 1969.

(29) John, P.; Odeh, I. M.; Thomas, M. J. K.; Tricker, M. J.; Wilson, J. I. B. *Phys. Status. Solidi B* **1981**, *105*, 499.

(30) He, L.; Inokuma, T.; Kurata, Y.; Hasegawa, S. *J. Non-Cryst. Solids* **1995**, *185*, 249.

(31) Low, H. C.; John, P. *J. Organomet. Chem*. **1980**, *201*, 363 and references therein.

(32) Wagner, C. D. Auger and X-ray Photoelectron Spectroscopy. In *Practical Surface Analysis*; Briggs, D., Seah, M. P., Eds.; Wiley: Chichester, 1994; Vol. 1, p 595.

Table 3. Stoichiometry[a] of the Solid Materials Photodeposited from $[(CH_3)_nH_{3-n}Si]_2O$ and of Their Residues after TGA

precursor	XPS analysis of solid material	EDX analysis of solid materials	XPS analysis of residue after TGA	EDX analysis of residue after TGA
$[(CH_3)H_2Si]_2O$	$Si_{1.0}O_{1.0}C_{2.7}$	$Si_{1.0}O_{0.56}C_{1.5}$	$Si_{1.0}O_{2.0}C_{0.3}$	$Si_{1.0}O_{2.2}C_{0.41}$
$[(CH_3)_2HSi]_2O$	$Si_{1.0}O_{1.0}C_{1.7}$	$Si_{1.0}O_{0.85}C_{1.3}$	$Si_{1.0}O_{1.9}C_{0.9}$	$Si_{1.0}O_{1.4}$
$[(CH_3)_3Si]_2O$	$Si_{1.0}O_{1.0}C_{2.4}$	$Si_{1.0}O_{0.41}C_{1.3}$	$Si_{1.0}O_{1.8}C_{0.4}$	

[a] ±10%.

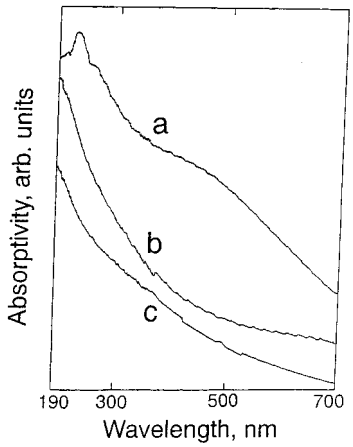

Figure 2. UV−vis absorption spectra of the solid materials from $[(CH_3)_2HSi]_2O$ (a), $[(CH_3)_3Si]_2O$ (b), and $[CH_3H_2Si]_2O$ (c).

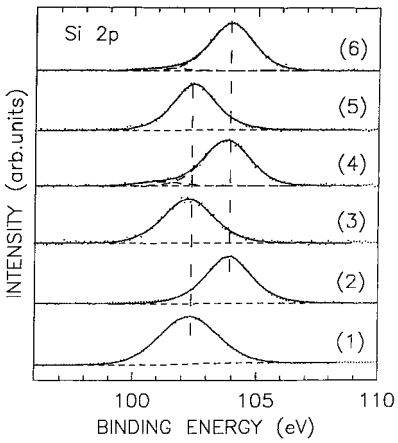

Figure 3. Si (2p) core level spectra of the solid materials from $[CH_3H_2Si]_2O$ (1), $[(CH_3)_3Si]_2O$ (3), and $[(CH_3)_2HSi]_2O$ (5) and of their residues produced upon TGA (2, 4, and 6, respectively).

takes place upon its transfer from the reactor to the spectrometer.

NMR Spectra. The ^{29}Si MAS NMR spectra of the deposited materials (Figure 4) consist of several peaks or broad bands assignable[33−35] to M (SiC_3O, 7−9 ppm), M_H ($SiHC_2O$, −6 to −8 ppm), X (SiC_4, 0 to −15 ppm), D (SiC_2O_2, −19 to −22 ppm), D_H ($SiHCO_2$, −32 to −37 ppm), T ($SiCO_3$, −55 to −64 ppm), T_H ($SiHO_3$, ∼ −85 ppm), and Q (SiO_4, −95 to −115 ppm) structural units. All the contributions are well manifested except for those of the M and M_H signals in the spectrum of the material from 1,3-dimethyldisiloxane (Figure 4a) where they contribute to a broad band. Relative importance of these structural units depends on the structure of the parent disiloxane; thus, the M units are most pronounced in the material from hexamethyldisiloxane, the M_H units are most significant in the material from 1,1,3,3-tetramethyldisiloxane, and the D_H units are of greatest magnitude in the material from 1,3-dimethyldisiloxane.

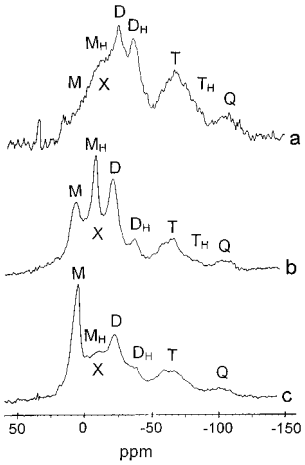

Figure 4. ^{29}Si MAS spectra of the solid materials obtained from $[CH_3H_2Si]_2O$ (a), $[(CH_3)_2HSi]_2O$ (b), and $[(CH_3)_3Si]_2O$ (c).

The ^{13}C NMR spectra of the deposited materials show only one line at 1.9 ppm belonging to $(CH_3)_nSi$ unit, which can include other signals, for example, a signal of $(Si)CH_2(Si)$ units is expected[34] in the region 1.6−3 ppm.

Electron Microscopy. SEM analysis shows that all the deposited materials have somewhat different morphology; bulkier agglomerates (size of several μm) are observed with those produced from 1,3-dimethyldisiloxane and hexamethyldisiloxane, while smaller bodies (size around 1 μm) are seen with that produced from 1,1,3,3-tetramethyldisiloxane (Figure 5). TEM analysis reveals that all agglomerates are composed of several tens of nm-sized interconnected chains. The illustration is given in Figure 6. The materials possess amorphous or nanocrystalline structure.

Thermal Analysis. Thermograms of the samples of the solid materials obtained from the photolysis of 1,3-dimethyldisiloxane, 1,1,3,3-tetramethyldisiloxane, and hexamethyldisiloxane are given in Figures 7−9. Generally, only methane, ethane, and ethyne were determined by gas chromatography. Thermal decomposition of the material from 1,1,3,3-tetramethyldisiloxane and hexamethyldisiloxane are one-stage processes giving rise to dark-gray solid residues of ca. 50 wt % of the initial sample, whereas that of the material from 1,3-dimethylsiloxane is a two-stage process leading to a dark-gray residue of ca. 77 wt % of the initial sample. The measured amounts of the three observed hydrocarbons (methane, ethane, and ethyne) (Figures 7−9, Table 4) account only for a small fraction of the thermally liberated material and indicate that the major fraction

(33) Beshah, K.; Mark, J. E.; Ackerman, J. *J. Polym. Sci., Part B* **1986**, *24*, 1207.
(34) Marsmann, H. In *NMR Basic Principles and Progress*; Diehl, P., Fluck, E., Kosfeld, R., Eds.; Springer-Verlag: Berlin, 1981; Vol. 17.
(35) Engelhardt, G.; Jancke, H.; Lipmaa, E.; Samoson, A. *J. Organomet. Chem*. **1981**, *210*, 295.

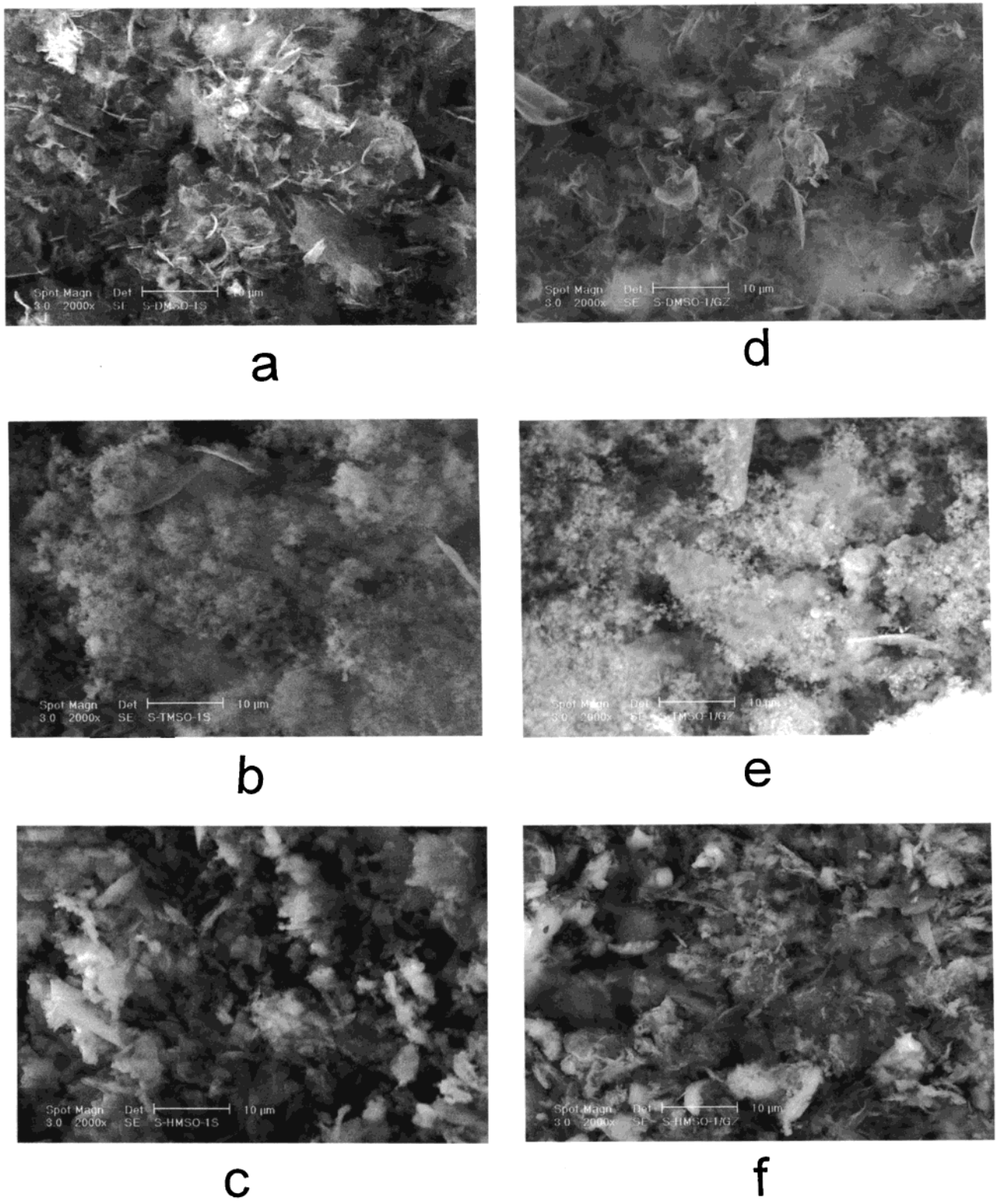

Figure 5. SEM images of the solid materials from $[CH_3H_2Si]_2O$ (a), $[(CH_3)_2HSi]_2O$ (b), $[(CH_3)_3Si]_2O$ (c) and of their residues produced upon TGA (d, e, and f, respectively).

must correspond to a portion of the sample evaporated, condensed below the hot zone and not passed to the gas chromatograph. We attempted to collect these materials, but succeeded only in one case. The FTIR spectrum of this liberated fraction from 1,1,3,3-tetramethyldisiloxane—wavenumber/cm^{-1} (normalized absorptivity): 622 (0.46), 693 (0.55), 774 (1.0), 831 (0.94), 1059 (0.42), 1132 (0.76), 1247 (0.58), 1409 (0.21), 2110 (0.46, 2788 (0.06), 2903 (0.46), 2942 (0.58) (Figure 10 a)—possesses merely a weak absorption at ν(SiO) (1059 cm^{-1}) and can be thus assigned neither to long-chained[28] $[(CH_3)_2SiO]_n$ nor to low-molecular-weight cyclic oligomeric siloxanes[36,37] but rather to a polycarbosilane with a low content of the Si−O bonds.

(36) Grassie, N.; MacFarlane, I. G. *Eur. Polym. J.* **1978**, *14*, 875.

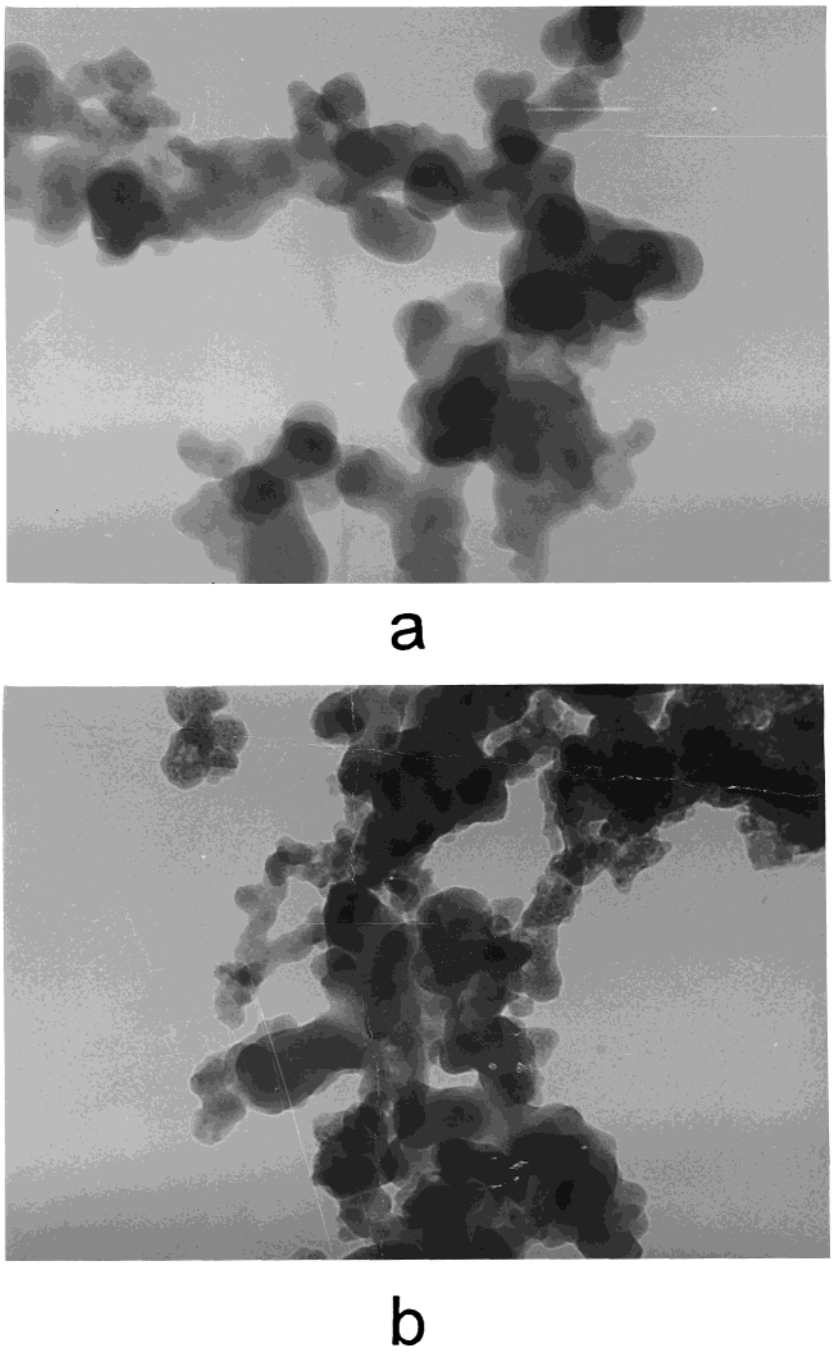

Figure 6. TEM image of the solid material from $[(CH_3)_2HSi]_2O$ (a) and its residue (b) (both magnification 100000 x).

The comparison of the decomposition profile in all three thermolyses (Figures 7−9) reveals that the most stable material is that from 1,3-dimethyldisiloxane: its degradation rate exhibits a shoulder at ca. 450 °C and the maximum at ca. 700 °C, whereas the degradation rate of the solids from 1,1,3,3-tetramethyldisiloxane and hexamethyldisiloxane has a maximum already at ca. 480 °C.

The other difference between the deposits is the way in which their decomposition maxima are related to the evolution of the hydrocarbons. The maximum degradation rate with the sample from 1,3-dimethylsiloxane coincides with the maximum evolution of methane, and the shoulder matches the maximum evolution of ethane (Figure 7). Conversely, the maximum degradation rate with the sample from 1,1,3,3-tetramethyldisiloxane (Figure 8) and hexamethyldisiloxane (Figure 9) precedes the maximum evolution of hydrocarbons. The far major hydrocarbon product with the deposits from 1,1-dimethyldisiloxane and 1,1,3,3-tetramethyldisiloxane is methane, but both methane and ethane are formed from the sample from hexamethyldisiloxane.

Properties of TGA Residues. Disregarding the different features of their formation, the residues from all three materials show very similar properties: the binding energy of Si (2p) electrons (Figure 3) is equal to 103.8 ± 0.1 eV which is 0.4 eV higher than that reported[32] for bulk SiO_2 and characteristic of highly dispersed silicon dioxide.[38] The prevailing Si^{4+} oxidation

(37) Fischer, C.; Kriegsmann, H. *Z. Anorg. Allg. Chem.* **1969**, *367*, 219.

(38) Miller, M. L.; Linton, R. W. *Anal. Chem.* **1985**, *57*, 2414.

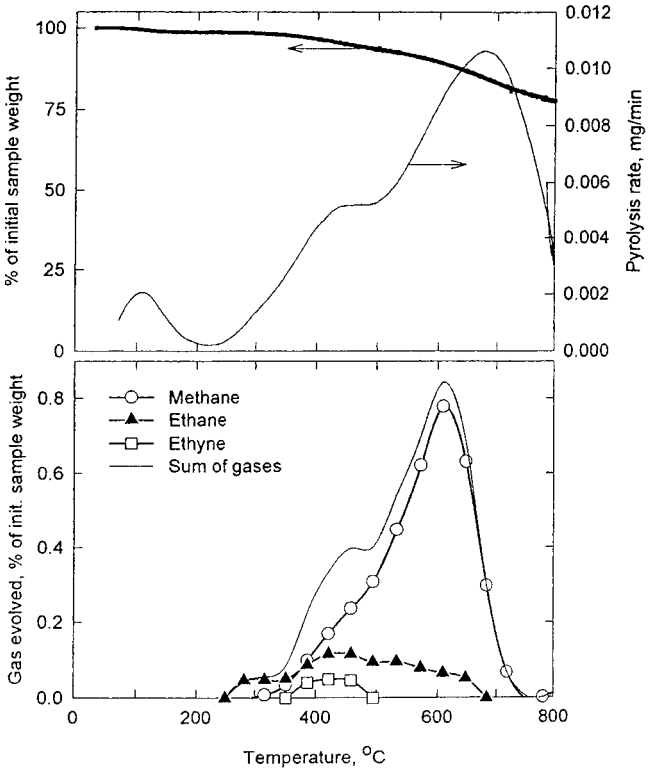

Figure 7. Thermal decomposition of the solid material obtained from 1,3-dimethyldisiloxane.

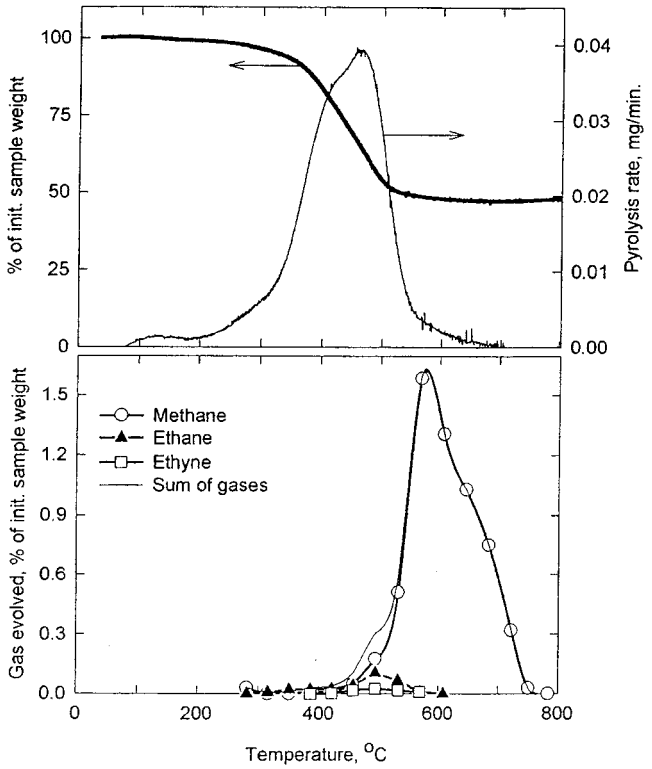

Figure 8. Thermal decomposition of the solid material obtained from 1,1,3,3-tetramethyldisiloxane.

state of silicon is in each case accompanied with very minor component (4−8%) with binding energy of Si (2p) electrons 100.6 ± 0.3 eV which can be assigned to silicon carbide.[32] The surface stoichiometry of the samples calculated from intensities of photoemission lines is consistent with SiO_2 accompanied with carbon whose

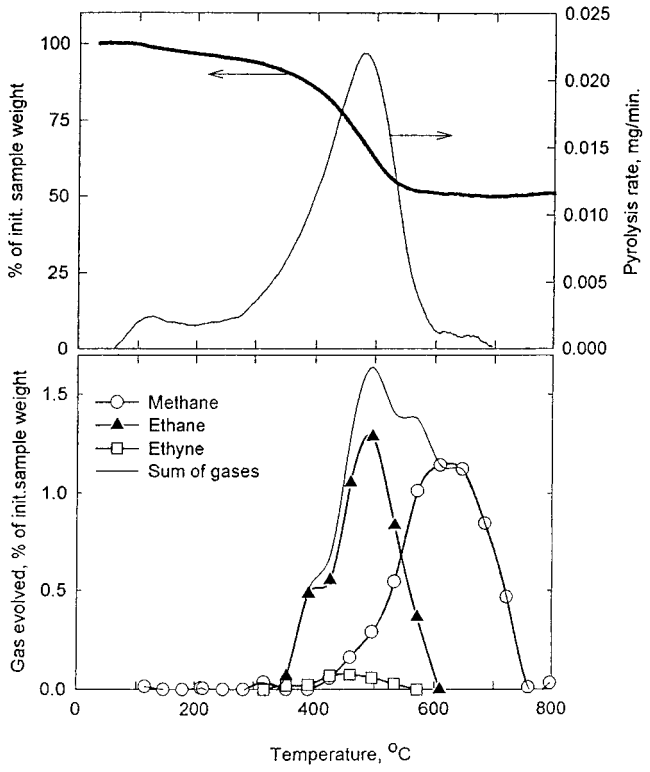

Figure 9. Thermal decomposition of the solid material obtained from hexamethyldisiloxane.

Table 4. Mass Balance of Thermal Decomposition of Solid Deposits

decomposition product, wt %	deposit from $[(CH_3)H_2Si]_2O$	deposit from $[(CH_3)_2HSi]_2O$	deposit from $[(CH_3)_3Si]_2O$
CH_4	3.69	5.74	5.70
C_2H_6	0.85	0.30	4.65
C_2H_2	0.14	0.07	0.28
gases in total	4.68	6.11	10.63
solid residue	77.23	48.07	53.31
liberated[a]	18.09	45.82	36.06

[a] Calculated to 100%.

content is between 0.3 and 0.9 of that of silicon (Table 3). Because of low quantities of these residues, EDX−SEM analysis was performed only with two samples (Table 3) and confirms that the heating of the deposited solids results in a decrease of carbon content and an increase of oxygen content in the bulk residues, which is in line with the data obtained from the XPS analysis for superficial layers. The increased oxygen content is likely caused by traces of oxygen in argon used as carrier gas.

FTIR spectra of the residues show the same pattern: Figure 10b shows bands of ν(Si−O) (1116 cm^{-1}), ν(Si−C) (824 cm^{-1}), $\delta(CH_3Si)$ (shoulder, 1228 cm^{-1}), ν(C═C) (1630 cm^{-1}), and ν(C−H) (2860 and 2922 cm^{-1}) vibrations, and it is in keeping with a mixture of SiO_2 (ν(Si−O) ∼1080 cm^{-1}, ref 39), SiC (ν(Si−C) near 800 cm^{-1}, ref 40), and a polysiloxane. They confirm that the residues are a mixture of silicon dioxide, silicon carbide, and a small amount of methylsilicone.

(39) Pai, P. G.; Chao, S. S.; Takagi, Y.; Lucovsky, G. *J. Vac. Sci. Technol., A* **1986**, *4*, 689 and references therein.
(40) For example, Ramis, G.; Quintard, P.; Cauchetier, M.; Busca, G.; Lorenzelli, V. *J. Am. Ceram. Soc.* **1989**, *72*, 1692.

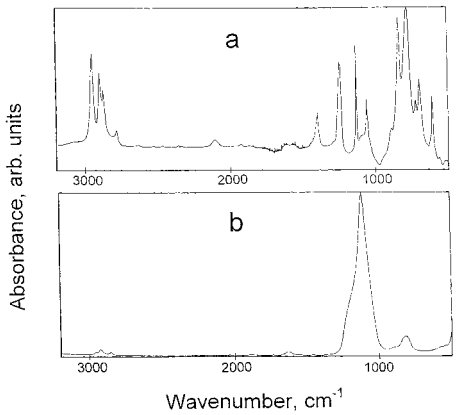

Figure 10. FTIR absorption spectrum of the evaporated/condensed fraction (a) and of the residue (b) obtained from TGA analysis of the solid material from 1,1,3,3-tetramethyldisiloxane.

SEM and TEM analysis of the residues show that the morphology patterns are retained upon heating (Figures 5 and 6).

4. Discussion

Photolysis Mechanism. The observed formation of hydrocarbons reveals cleavage of the Si−C and Si−H bonds and that of methylsilanes confirms cleavage of the Si−O bond. The XPS, FTIR, and NMR show that the solid products are polysiloxanes possessing less Si−H bonds than their precursors and having all possible (M, M_H, X, D, D_H, T, T_H, and Q) tetrahedral structures.

The energy delivered by the photons at 193 nm corresponds to ca. 620 kJ mole^{-1}, which is much[41] in excess of the energy needed for cleavage of the weaker Si−C (ca. 370 kJ mole^{-1}), C−H (ca. 410 kJ mole^{-1}), and Si−H (ca. 380 kJ mole^{-1}) bonds, of the strongest Si−O bond (ca. 530 kJ mole^{-1}) bond, and also for inducing three-center elimination of silylenes and carbenes (∼250−300 kJ mole^{-1}, refs 42−44).

Hence, the formation of the observed products can take place via (a) homolysis of the Si−X (X = C, H, O) bonds, (b) via silylenes (and carbenes) eliminations, and (c) via Si−C/Si−O and Si−H/Si−O scrambling.

The occurrence of all these channels, which would make the total reaction scheme complex, is supported by available literature data on photolytic and thermal reactions of similar molecules and on reactivity of transient species.

Relative amounts of CH_4, C_2H_2, and C_2H_6 in the photolysis of each of the $[(CH_3)_nH_{3-n}]_2O$ are different, but the surprisingly similar yields of methane for each n can be only explained as associated with three plausible channels to this compound, which are 1,1-[CH_4] expulsion and H(Si) and H(C) abstraction by the CH_3 radical. The observed ethane, ethene, and ethyne can result from the known reactions 2 $CH_3\bullet \rightarrow C_2H_6$, $CH_3\bullet \rightarrow :CH_2 + H$, 2 $:CH_2 \rightarrow C_2H_4$, $C_2H_4 \rightarrow C_2H_2 + H_2$. The yield of ethane decreases when going from $n = 3$ via $n = 1$ to $n = 2$. It can reflect different extent of the CH_3 radical recombination and concerted 1,1-[C_2H_6] elimination. The operation of the latter channel (e.g., refs 45 and 46) with $(CH_3)_2HSiOSi(CH_3)_2H$ and especially with $(CH_3)_3SiOSi(CH_3)_3$ can be facilitated by the presence of an excess of energy after absorption of laser photon(s). The very different yields of ethyne, a high-temperature product, may be related to two different channels for this product—ethene dehydrogenation and $:CH_2$ extrusion from the Si−CH_3 bond—which differ with each n.

The anticipated primary processes in the photolysis are 1,1-[H_2] and 1,1-[CH_4] extrusions[47,48] yielding silylenes $(CH_3)_nH_{3-n}SiO(CH_3)_{n-1}H_{2-n}Si:$ and $(CH_3)_nH_{3-n}$-$SiO(CH_3)_nH_{1-n}Si:$ which can insert into the Si−H bonds of the parent compounds and combine to unstable[49] disilenes undergoing a number of addition and rearrangement reactions. These reactions apply only to the disiloxanes with $n = 1, 2$ and would finally produce siloxanes with Si−Si bonds and with M or M_H units.

The Si−O bond cleavage is a difficult primary photochemical event[21,22] but can be feasible in radicals produced from the disiloxanes through the Si−C and Si−H bond fissions (eqs 1, 2).

$$[(CH_3)_nH_{3-n}Si]_2O \xrightarrow[-CH_3\bullet]{} (CH_3)_{n-1}H_{3-n}\dot{S}i{-}O{-}Si(CH_3)_nH_{3-n} \quad (1)$$

$$[(CH_3)_nH_{3-n}Si]_2O \xrightarrow[-H\bullet]{} (CH_3)_nH_{2-n}\dot{S}i{-}O{-}Si(CH_3)_nH_{3-n} \quad (2)$$

These secondary reactions (eqs 3, 4)

$$(CH_3)_{n-1}H_{3-n}\dot{S}i{-}O{-}Si(CH_3)_nH_{3-n} \rightarrow (CH_3)_{n-1}H_{3-n}Si{=}O + \dot{S}i(CH_3)_nH_{3-n} \quad (3)$$

$$(CH_3)_nH_{2-n}\dot{S}i{-}O{-}Si(CH_3)_nH_{3-n} \rightarrow (CH_3)_nH_{2-n}Si{=}O + \dot{S}i(CH_3)_nH_{3-n} \quad (4)$$

yield silanones and small Si-centered radicals which can disproportionate[50,51] into reactive silenes and methylsilanes. Ensuing silene isomerization into silylenes[49] and reaction of silylenes[43] with H_2 can yield the observed methylsilanes $(CH_3)_nSiH_{4-n}$. The silanones produced (eqs 3 and 4) polymerize and insert into Si−H bonds.[49] The silanone polymerization (eq 5) would finally lead

$$n(CH_3)_nH_{2-n}Si{=}O \rightarrow -[(CH_3)_nH_{2-n}Si{-}O]n \quad (5)$$

to siloxanes with M and M_H units; their insertion into

(41) Walsh, R. In *The Chemistry of Organic Silicon Compounds;* Patai, S., Rappoport Z., Eds.; Wiley: Chichester, U.K., 1989; Chapter 5.
(42) Jasinski, J. M.; Estes, R. D. *Chem. Phys. Lett.* **1985**, *117*, 495.
(43) Jasinski, J. M.; Becerra, R.; Walsh, R. *Chem. Rev.* **1995**, *95*, 1203.
(44) Benson, S. W. *Thermochemical Kinetics*; Wiley: New York, 1976.
(45) Fahr, A.; Braun, W.; Klein, R.; Dorko, W.; Okabe, H. *J. Chem. Soc., Faraday Trans.* **1991**, *87*, 2383.
(46) Pola, J.; Taylor, R. *J. Organomet. Chem.* **1992**, *437*, 271.
(47) Rickborn, S. E.; Ring, M. A.; O'Neal, H. E.; Coffey, D. *Int. J. Chem. Kinet.* **1984**, *16*, 289.
(48) Pola, J.; Taylor, R. *J. Organomet. Chem.* **1993**, *446*, 131 and references therein.
(49) Raabe, G.; Michl J. In *The Chemistry of Organic Silicon Compounds;* Patai, S., Rappoport Z., Eds.; Wiley: Chichester, U.K., 1989; Chapter 17.
(50) Tokach, S. K.; Koob, R. D. *J. Am. Chem. Soc.* **1980**, *102*, 376.
(51) Gammie, L.; Safarik, I.; Strausz, O. P.; Roberge, R.; Sandorfy, C. *J. Am. Chem. Soc.* **1980**, *102*, 378.

Si−H bonds of the parent disiloxanes and intermediates results in the formation D, D_H,T, and T_H structures (eq 6).

$$(CH_3)_nH_{3-n}Si-O-\underset{|}{\overset{|}{Si}}-H \xrightarrow{(CH_3)_nH_{2-n}Si=O} (CH_3)_nH_{3-n}Si-O-\underset{|}{\overset{|}{Si}}-O-SiH_{2-n}(CH_3)_n \quad (6)$$

The observation of Q units in all the final deposited materials can be only explained by scrambling of Si−C and Si−O bonds, which does not occur in solution[52] but was suggested to take place in the solid state.[4,53,54] These reactions must be particularly important in the photolysis of hexamethyldisiloxane.

Other possible reactions are redistribution of Si−H and Si−O bonds[55,56] and the Yajima rearrangement[57] in siloxanes with (CH_3)Si−Si bond into siloxanes with (H)Si−CH_2−Si link.

The very specific feature of all these reactions is that the macromolecular products are produced within periods shorter than 1 ms (see e.g., refs 58 and 59) and that these reactions take place in the small region of the gas phase restricted by the laser beam at room temperature of the total gaseous volume.

Thermal Decomposition of Solid Materials. The formation of methane during thermolysis of the material from 1,3-dimethyldisiloxane and 1,1,3,3-tetramethyldisiloxane and that of methane and ethane during thermolysis of the material from hexamethyldisiloxane can be rationalized in terms of formation of methane by combination of CH_3 radicals with H atoms and in terms of formation of ethane by combination of CH_3 radicals; both Si−H and Si−CH_3 groups are available only in the former samples. The preponderance of methane over ethane in the thermolysis of the materials from $[(CH_3)_nH_{3-n}Si]_2O$ ($n = 1, 2$) is in keeping with lower barrier for methane formation, which is due to latent Si−H bonds. The formation of methane in the thermolysis of the deposit from $[(CH_3)_3Si]_2O$ follows the formation of ethane. It is possible that methane is produced from the liberated fraction formed above the hot zone.

It is appropriate to relate the observed thermal behavior of the deposited materials to thermal degradation of conventionally prepared polysiloxanes, which is different for linear, branched-chain, and cross-linked siloxanes.

Poly(dimethylsiloxane)s of the M−D_y−M type[36,60−62] and various substituted $(R_1R_2SiO)_n$ polysiloxanes[63] start to decompose via molecular rearrangement at ca. 350 °C and reach maximum decomposition rate in a dynamic atmosphere of nitrogen at ca. 440 °C (ref 36). The principal products of these decompositions are cyclic oligomers $(R_2SiO)_n$. Hydrocarbon products were not observed at all, and polysiloxane residues having IR spectrum indistinguishable[36] from that of the starting polysiloxanes can be totally volatilized by prolonged heating above 400 °C.

Branched-chain $M_xD_yT_z$ polymethylsiloxanes undergo[64] thermal depolymerization−volatilization similar to M−D_y−M siloxanes. The degradation weight losses vary inversely with the level of chain branching and the T content increases in the residue and dominates its structure.

Highly cross-linked polysiloxanes[65] begin to degrade at temperatures above 400 °C and show their maximum decomposition rates at temperatures above 520 °C. They do not evolve any Si−O containing products but hydrogen and hydrocarbons and maintain the initial silicon neighborhood unscrambled[6] up to about 500 °C. Low temperature heating (400−600 °C) yields up to ca. 30% of weight loss, and the key feature for obtaining SiC from these siloxanes is heating to above 1600 °C and having enough carbon to allow CO evolution (e.g., refs 66 and 67).

Considering these features, the observed thermal behavior of the photodeposits reveals that the photodeposits are more stable than linear poly(dialkylsiloxanes). This suggests that they have branched chains. The observation of the small yield of the C_1−C_2 hydrocarbon products indicates that the deposits are partly cross-linked.

5. Conclusion

ArF laser gas-phase photolysis of methyldisiloxanes $[(CH_3)_nH_{3-n}Si]_2O$ ($n = 1-3$) yields C_1−C_2 hydrocarbons (major volatile products), methylsilanes (minor volatile products), and solid methylsilicones with their structures (the Si/O ratio, Si−H bond content) reflecting that of the parent disiloxanes. Volatile products are compatible with primary photolytic cleavage of the Si−C and Si−H bonds along with cleavage of the Si−O bonds in intermediate Si-centered radicals. The deposited solid nano-textured materials show less H(Si) centers than their precursors and contain M, M_H, X, D, D_H, T, T_H, and Q units which are presumed to be formed by insertion of intermediate silanone into Si−H bonds or Si−C/SiO and Si−H/Si−O scrambling reactions. The multitude of reactions leading to the solid hydrido(methyl)silicones, normally requiring high temperatures, take place within less than 1 ms in a small region of gas phase which is restricted by the laser beam. At these conditions, room temperature of total gaseous volume is maintained, and the procedure allows deposi-

(52) Moedritzer, K. *Organomet. Chem. Rev*. **1966**, *1*, 179.
(53) Belot, V.; Corriu, R. J. P.; Leclercq, D.; Mutin, P. H.; Vioux, A. *J. Mater. Sci. Lett*. **1990**, *9*, 1052.
(54) Burns, G. T.; Taylor, R. B.; Xu, Y.; Zangvil, A.; Zank, G. A. *Chem. Mater*. **1992**, *4*, 1313.
(55) Belot, V.; Corriu, R. J. P.; Leclercq, D.; Mutin, P. H.; Vioux, A. *J. Non-Cryst. Solids* **1992**, *144*, 287.
(56) Belot, V.; Corriu, R. J. P.; Leclercq, D.; Mutin, P. H.; Vioux, A. *Chem. Mater*. **1991**, *3*, 127.
(57) Yajima, S.; Hasegawa, Y.; Hayashi, J.; Iimura, M. *J. Mater. Sci*. **1978**, *13*, 2569.
(58) Dhanya, S.; Kumar, A.; Vatsa, R. K.; Saini, R. D.; Mittal, J. P.; Pola, J. *J. Chem. Soc., Faraday Trans*. **1996**, *92*, 179.
(59) Vatsa, R. K.; Kumar, A.; Naik, P. D.; Upadhyaya, H. P.; Pavanaja, U. B.; Saini, R. D.; Mittal, J. P.; Pola, J. *Chem. Phys. Lett*. **1996**, *255*, 129.
(60) Patnode, N.; Wilcock, D. F. *J. Am. Chem. Soc*. **1946**, *68*, 358.
(61) Lewis, C. W. *J. Polym. Sci*. **1958**, *33*, 153.
(62) Thomas, T. H.; Kendrick, T. C. *J. Polym. Sci., A2*, **1969**, *7*, 537.
(63) Thomas, T. H.; Kendrick T. C. *J. Polym. Sci., A2*, **1970**, *8*, 1823.
(64) Nielsen, J. M. *J. Appl. Polym. Sci., Appl. Polym. Symp*. **1979**, *35*, 223.
(65) Wilson, A. M.; Zank, G.; Euguchi, K.; Xing, W.; Yates, B.; Dahn, J. R. *Chem. Mater*. **1997**, *9*, 1601.
(66) Taylor, R. B.; Zank, G. A. *Polym. Prepr. (Am. Chem. Soc., Div. Polym. Chem.)* **1991**, *32*, 586.
(67) White, D. A.; Oleff, S. M.; Fox, J. R. *Adv. Ceram. Mater*. **1987**, *2*, 53.

tion of the methylsilicones on cold substrates. The nanostructured hydrido(methyl)silicones are thermally more stable than conventionally prepared linear poly(dialkylsiloxanes), and their thermolytic features are in keeping with partly branch-chained and partly cross-linked structures.

Acknowledgment. We thank GAAVCR of the Czech Republic (grant no. A4072806) and STA of Japan for support.

CM011109O